Hedgehog pathway inhibitors of the acylthiourea and acylguanidine class show antitumor activity on colon cancer in vitro and in vivo

Accepted Manuscript

Hedgehog pathway inhibitors of the acylthiourea and acylguanidine class show antitumor activity on colon cancer in vitro and in vivo

Loredana Vesci, Ferdinando Maria Milazzo, Maria Antonietta Stasi, Silvia Pace, Francesco Manera, Carlo Tallarico, Elena Cini, Elena Petricci, Fabrizio Manetti, Rita De Santis, Giuseppe Giannini

PII: S0223-5234(18)30619-6

DOI: 10.1016/j.ejmech.2018.07.053

Reference: EJMECH 10588

To appear in: *European Journal of Medicinal Chemistry*

Received Date: 7 June 2018

Revised Date: 19 July 2018

Accepted Date: 22 July 2018

Please cite this article as: L. Vesci, F.M. Milazzo, M.A. Stasi, S. Pace, F. Manera, C. Tallarico, E. Cini, E. Petricci, F. Manetti, R. De Santis, G. Giannini, Hedgehog pathway inhibitors of the acylthiourea and acylguanidine class show antitumor activity on colon cancer in vitro and in vivo, *European Journal of Medicinal Chemistry* (2018), doi: 10.1016/j.ejmech.2018.07.053.

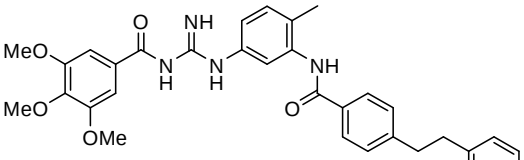

5

Luc inhibition (Shh-lightII cells): IC_{50} = 20 nM
ALP inhibition (C3H10T1/2 cells): IC_{50} = 40 nM
Growth inhibition (LS180 cells): EC_{50} = 2.5 µM
Growth inhibition (HT1080 cells): EC_{50} = 2.0 µM
Good PK parameters

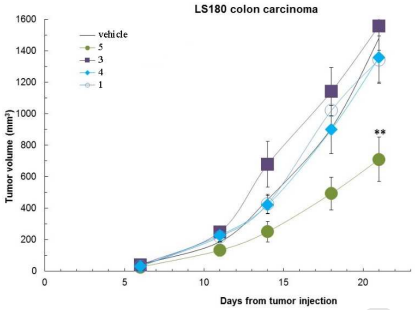

Hedgehog pathway inhibitors of the acylthiourea and acylguanidine class show antitumor activity on colon cancer in vitro and in vivo

Loredana Vesci,[a]^ Ferdinando Maria Milazzo,[a]^ Maria Antonietta Stasi,[a] Silvia Pace,[a] Francesco Manera,[a] Carlo Tallarico,[a] Elena Cini,[b,c] Elena Petricci,[c*] Fabrizio Manetti,[b,c] Rita De Santis,[a] and Giuseppe Giannini[a]*

[a]*Research & Development, Alfasigma SpA, via Pontina, km 30.400, I-00040 Pomezia, Italy*

[b]*Lead Discovery Siena Srl, via Fiorentina 1, I-53100 Siena, Italy*

[c]*Dipartimento di Biotecnologie, Chimica e Farmacia, Università di Siena, Dipartimento di Eccellenza 2018-2022, via A. Moro 2, I-53100 Siena, Italy*

Loredana Vesci: loredana.vesci@alfasigma.com
Ferdinando Maria Milazzo: ferdinando.milazzo@alfasigma.com
Maria Antonietta Stasi: mariaantonietta.stasi@alfasigma.com
Silvia Pace: silvia.pace@alfasigma.com
Francesco Manera: francesco.manera@alfasigma.com
Carlo Tallarico: carlo.tallarico@alfasigma.com
Elena Cini: cinielena@libero.it
Elena Petricci: elena.petricci@unisi.it
Fabrizio Manetti: fabrizio.manetti@unisi.it
Rita De Santis: rita.desantis@alfasigma.com
Giuseppe Giannini: giuseppe.giannini@alfasigma.com

^These two authors equally contributed to this work

*****Corresponding author: Dr. Giuseppe Giannini, phone: +39 06 91393640, email: giuseppe.giannini@alfasigma.com; Dr. Elena Petricci, phone: +39 0577 234276, email: elena.petricci@unisi.it.

Abstract. Small series of acylguanidine and acylthiourea derivatives were synthesized in gram-scale and assayed for their ability to modulate the Hh signalling pathway. In vitro studies showed a low micromolar inhibitory activity toward tumor cell lines, while the oral administration revealed an excellent ADME profile in vivo. Compound **5** emerged as the most active and safe inhibitor of colon cancer cells both in vitro and in a xenograft mouse model. Based on these data, **5** could be prioritized to further development with the perspective of clinical studies.

Keywords: Hedgehog inhibitor; in vivo pharmacokinetics; gram-scale synthesis; ADME-Tox; LS180 xenograft; acylguanidine.

1. Introduction[1]

The Hedgehog (Hh) signalling pathway, which is active in early embryonic development, plays a pivotal role in regulation of cell proliferation and differentiation, by controlling the correct maturation of developing tissues [1, 2]. In adulthood, Hh signalling is active in early progenitor cells, whereas aberrant activation of the Hh pathway is associated with the development of malignant transformation in a variety of human cancers [3]. The pathway can be stimulated by three ligands: Sonic Hedgehog (Shh), Indian Hedgehog, and Desert Hedgehog. When one of these ligands binds to Patched (Ptch), a 12-pass transmembrane protein that functions as a repressor of the pathway, the inhibition of the downstream transmembrane receptor Smoothened (Smo) by Ptch itself is relieved. Activated Smo in turn initiates a downstream signalling cascade leading to the activation of Gli transcription factors (Gli-1, -2, -3). They translocate into the nucleus and induce transcription of Gli target genes, such as *Gli-1* itself, *Ptch1* (the gene encoding the Hh-interacting protein), *Bcl2*, D-type cyclins, *c-Myc*, *Snail* and *BMI1*, all having a pro-tumorigenic role [4]. Ligand-independent mechanisms can also be responsible for the constitutive Hh pathway activity in cancers. Ligand-independent constitutive activation of the Hh pathway, found in basal cell carcinoma (BCC) and medulloblastoma, is characterized by the presence of somatic mutations in *Ptch1*, *Smo* or *SUFU* genes [5]. On the other hand, the ligand-dependent activation observed in a wide range of cancers including melanoma, pancreatic, lung, breast, renal, and colorectal cancers [1, 3], is associated with elevated production of Hh ligands by tumor or stromal cells [2]. In all cases, the activated Hh signalling leads to increased cell proliferation and neoplastic transformation.

Anticancer therapy based on the inhibition of Hh signalling has been clinically validated with two new drugs approved by FDA in 2012 and 2015 for the treatment of adult BCC [6, 7]: GDC-0449 (vismodegib, Erivedge™ by Roche, **1**, Figure 1) [8] and NVP-LDE225 (erismodegib, also known as sonidegib, Odomzo™ by Novartis, **2**) [9]. Both of them are Smo inhibitors, act by direct interaction with the protein, and share a common diaryl carboxamide chemical scaffold.

[1]Abbreviations: Hh, Hedgehog; Shh, Sonic Hedgehog; Ptch, Patched; Smo, Smoothened; BCC, basal cell carcinoma; PE, petroleum ether; SRB, sulforhodamine B; Shh-CM, Shh-conditioned media; TV, tumor volume; TUI, tumor volume inhibition; BWL, body weight loss; HBSS, Hank's balanced salt solution; RLU, Relative Light Unit; ALP, alkaline phosphatase; SAG, Smo agonist; MW, microwave; 7-ETC, 7-ethoxy coumarin; Gli, glioma-associated oncogene; I/E, influx/efflux.

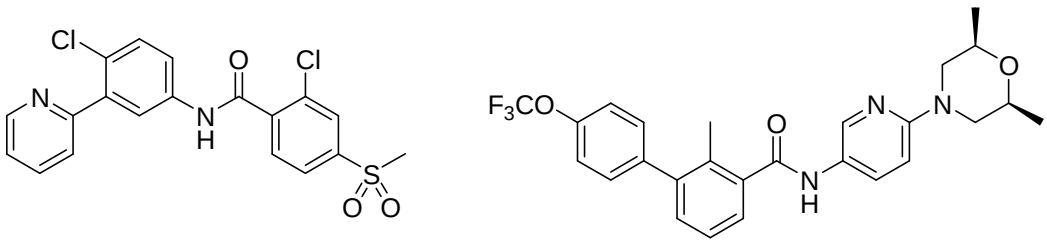

GDC-0449, vismodegib (Erivedge^{TM}), **1** erismodegib, sonidegib (Odomzo^{TM}), **2**

Figure 1. FDA-approved Smo antagonists.

Compound **1** is a small Smo antagonist able to block intracellular signalling pathway upon binding to Smo, thus resulting in inhibition of *Gli-1* and down-modulation of related target genes. Because the activated Hh pathway found in BCC is shared with other types of tumors, **1** is currently under investigation in 61 active and completed clinical trials targeting medulloblastoma, chondrosarcoma, pancreatic, small-cell lung, gastric cancer and colorectal cancer [10, 11].

In a similar way, **2** is involved in 28 active and completed clinical trials for prostatic, ovarian, pancreatic, breast, and esofageal cancer, as well as medulloblastoma and other tumors [11].

Moreover, there are currently three additional Smo inhibitors in clinical trials (namely, PF-04449913, LY2940680, and itraconazole) [11]. Extensive pre-clinical investigations are ongoing worldwide on Smo because it is recognized as a particularly appealing target for its central role in the regulation of the Hh signalling pathway and for its easy accessibility on the tumor cell surface [12]. Unfortunately, cell lines that exhibit the presence of Smo variants and are resistant to **1** already appeared [13-15]. In this context, although **2** seems to represent an effective alternative treatment to **1** in resistant tumors, new additional small molecules able to modulate the Hh pathway are urgently needed.

Our research group is strongly involved in the search of novel inhibitors of the Hh pathway [16-23] and/or Smo agonists [24, 25]. In this paper, we show that preliminary in vitro experiments on acylguanidine and acylthiourea Smo inhibitors, synthesized at lab scale, allowed us to identify four candidates (Table 1) that were then prepared in larger scale (5-7 g) for further pharmacological characterization. An ADME-Tox study was then performed to evaluate their drug-likeness, followed by an in vivo pharmacokinetic profiling and administration in a xenograft colon cancer mouse model. Following a classical medicinal chemistry approach, the overall experimental protocol was applied to eventually prioritize one or more compounds to access clinical trials. Three of these compounds (namely, **3**-**5**) belong to the acylguanidine class previously disclosed [16, 17, 21], while **6** is a new acylthiourea derivative. They have a common 3,4,5-trimethoxybenzoyl terminal fragment (thereafter referred to as region A, Figure 2), and an

acylguanidine or an acylthiourea moiety as the core portion linked to a second terminal aryl carboxamide fragment (region B).

The acylthiourea **6** and its corresponding acylguanidine analogue **3** were specifically selected to investigate the influence of the core portion on ADME properties and in vivo activity. Moreover, for a better understanding of the impact of the fluorine atom on the biological profile, the unsubstituted analogue **4** was also selected. Finally, previous results on leukemia and melanoma cells showed a remarkable in vitro [17, 18] and in vivo activity [19] of **5** (the guanidine derivative bearing a phenylethyl group in 4 position of the region B), thus prompting us to include this compound in our present investigation.

Figure 2. General structure of the studied compounds.

Table 1. Selected compounds tested as putative Smo inhibitors.

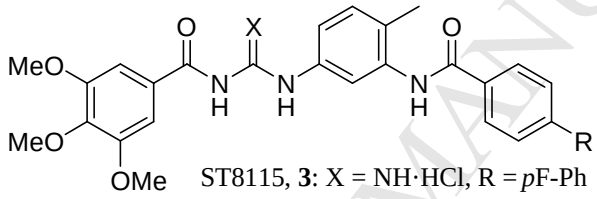

ST8115, **3**: X = NH·HCl, R = *p*F-Ph
ST8117, **4**: X = NH·HCl, R = Ph
ST8116, **5**: X = NH·HCl, R = -$(CH_2)_2$-Ph
ST8113, **6:** X = S, R = *p*F-Ph

Experimental results presented here confirm that compounds with an acylguanidine core are more active than the corresponding acylthiourea analogues (compare **3** with **6**), and a flexible molecular edge as in **5** is preferred to a rigid biphenyl moiety. Overall, **5** emerges as the best lead candidate among test compounds and deserves further development efforts as a new oral Hh inhibitor.

2. Materials and Methods

2.1. Chemistry

All reagents were used as purchased from commercial suppliers without further purification. Reactions were carried out in oven-dried or flamed vessels. Solvents were dried and purified by conventional methods prior use. All MW-assisted reactions were performed in a CEM Discover microwave oven equipped with a 35 mL tube for reactions under pressure and an external IR sensor to detect the reaction temperature during the irradiation (CEM Corporation, Cologno al Serio, Italy). Flash column chromatography was performed with Aldrich silica gel 60, 0.040-0.063 mm (230-400 mesh). Aldrich aluminum backed plates pre-coated with silica gel 60 (UV254) were used for analytical thin layer chromatography and were visualized by staining

with a $KMnO_4$, Pancaldi, or ninidrine solution. NMR spectra were recorded at 25 °C and 400 or 300 MHz for ^1H and 100 or 75 MHz for ^{13}C. The solvent is specified for each spectrum. Splitting patterns are designated as s, singlet; d, doublet; t, triplet; q, quartet; m, multiplet; br, broad. Chemical shifts (δ) are given in ppm relative to the resonance of their respective residual solvent peaks. High and low resolution mass spectroscopy analyses were recorded by electrospray ionization.

*Synthesis of (E)-4-styrylbenzoic acid **10**.* To a solution of 4-iodobenzoic acid **7** (1.5 g, 6 mmol, 1 equiv) and styrene **8** (2.7 mL, 24 mmol, 4 equiv) in DMF (10 mL), **9** (39 mg, 0.06 mmol, 0.01 equiv) and Et_3N (1.2 mL, 8.4 mmol, 1.4 equiv) were added. The reaction mixture was irradiated with MW in open vessel conditions, at 110 °C for 20 min (maximum power 150 W). Compound **8** (0.67 mL x 2, 6 mmol x 2, 1 equiv x 2) was added and the reaction was irradiated with MW in the same conditions twice. Water (50 mL) was added, followed by 1N HCl until pH 2. The white precipitate formed was filtered over Büchner, washing with H_2O (50 mL) and petroleum ether (PE, 2 x 50 mL). The pale rose solid obtained (1.5 g) was purified by flash chromatography using $CHCl_3/CH_3OH$ (9:1) as the eluent thus leading to a white solid (1.1 g) in 82% yield. ^1H NMR (400 MHz, DMSO-d_6) δ 12.75 (bs, 1H), 7.96 (d, J = 8 Hz, 2H), 7.72 (d, J = 8 Hz, 2H), 7.64 (d, J = 7.6 Hz, 2H), 7.45–7.26 (m, 11H). ^{13}C NMR (100 MHz, DMSO-d_6) δ 131.41, 130.21, 129.23, 128.63, 127.77, 127.27, 126.92. ES-MS: 223 $[M - H]^-$.

*Synthesis of (E)-4-styrylbenzoyl chloride **11***. The acid **10** (3 g, 13.4 mmol, 1 equiv) was dissolved in CH_2Cl_2 (220 mL), and oxalyl chloride (5.6 mL, 67 mmol, 5 equiv) and DMF (730 μL) were added. The reaction mixture was stirred at rt for 3 h. The solvent was removed under reduced pressure and the solid obtained was directly used for the next step without further purification and characterization.

*General procedure for the synthesis of nitro derivatives **13** and **17a-b**.* The proper acylchloride (**11** or **16a-b**, 9.2 mmol, 1.2 equiv) was dissolved in dry CH_2Cl_2 (50 mL) and the solution was cooled down to 0 °C. 2-Methyl-5-nitro aniline **12** (1.17 g, 7.7 mmol, 1 equiv) and pyridine (1.2 mL, 15.4 mmol, 2 equiv) were added. After 10 min, the reaction mixture was heated up to rt and stirred overnight under N_2. After dilution with CH_2Cl_2 (50 mL), the reaction mixture was washed with 1N HCl (3 x 30 mL), a saturated solution of $NaHCO_3$ (3 x 30 mL), and brine (2 x 30 mL). The organic phase was dried over dry Na_2SO_4 and, after filtration and evaporation under reduced pressure, the crude product was purified by flash chromatography.

*General procedure for the synthesis of **14** and **18a-b**.* To a solution of **13** or **17a-b** (5 mmol, 1 equiv) in MeOH (30 mL), Pd/C 5% (0.2 mmol, 0.05 equiv) was added under N_2. After 3 N_2/vacuum cycles, the reaction mixture was stirred at rt under H_2 overnight. The suspension was

filtered over a Celite pad and washed with MeOH (3 x 50 mL). The solvent was removed under reduced pressure and the product directly used without further purification.

*General procedure for the synthesis of **15** and **19a-b**.* To solution of the proper aniline (**14** or **18a-b**, 4.1 mmol, 1 equiv) in MeOH (2.5 mL), a 10% HCl solution in MeOH (7.5 mL) was added. The mixture was stirred at rt under N_2 overnight. The precipitate formed during the night was directly used without further purification and characterization.

*Synthesis of 4'-fluoro-N-(2-methyl-5-(3-(3,4,5-trimethoxybenzoyl)thioureido)phenyl)-[1,1'-biphenyl]-4-carboxamide (**6**).* 3,4,5-Trimethoxybenzoyl chloride **20** (2.4 g, 10.4 mmol, 1 equiv) was dissolved in dry acetone (200 mL) and NH_4SCN (858 mg, 11.2 mmol, 1.2 equiv) was added. The suspension obtained was stirred at reflux for 2 h and **18b** (3 g, 9.4 mmol, 1 equiv) was added. The reaction mixture was refluxed for additional 3 h under N_2 and directly poured into a backer previously filled with ice. The solid formed was filtered in a Büchner funnel and washed with H_2O (2 x 40 mL), and PE (2 x 40 mL). The solid was finally purified by flash chromatography (AcOEt/PE: 4:1) obtaining a pale yellow solid in 67% yield. ^{1}H NMR (400 MHz, $CDCl_3$) δ 12.54 (bs, 1H), 9.05 (bs, 1H), 8.32 (ds, *J* = 2.2 Hz, 1H), 7.93 (d, *J* = 8.0 Hz, 2H), 7.78 (s, 1H), 7.63 (d, *J* = 7.9 Hz, 2H), 7.57-7.54 (m, 2H), 7.47, 7.46 (dd, J_1 = 8.2 Hz, J_2 = 2.2 Hz, 1H), 7.25 (s, 1H), 7.12 (t, *J* = 8.5 Hz, 2H), 7.05 (s, 2H), 3.91 (s, 9H), 2.32 (s, 3H). ^{13}C NMR (100 MHz, DMSO, d_6) δ = 179.1, 167.5, 1656.1, 160.5, 152.8, 142.5, 141.7, 136.7, 135.6, 135.5, 133.1, 131.7, 130.3, 129.0, 128.9, 128.8, 126.6, 122.0, 121.8, 116.0, 115.9, 115.7, 106.4, 60.2, 56.2, 17.6. Mp: 215-217 °C. Elemental analysis for $C_{31}H_{28}FN_3O_5S$ calc.: C, 64.91; H, 4.92; F, 3.31; N, 7.33; O, 13.95; S, 5.59; found: C, 64.94; H, 4.94; N, 7.32; S, 5.55.

*Synthesis of N-cyano-3,4,5-trimethoxybenzamide **21**.* 3,4,5-Trimethoxybenzoyl chloride **20** (0.026 mol, 1 equiv) was suspended in Et_2O (30 mL), and a solution of NH_2CN (0.026 mol, 1 equiv) in 10% aqueous NaOH (26 mL) was added at 0 °C. The reaction mixture was stirred at rt for 1 h, then cooled down to 0 °C, and 1N HCl was added until pH 2. The white solid obtained was dissolved in AcOEt at reflux, then PE was added until full precipitation. After filtration over Büchner and washing with PE, a white solid was obtained. ^{1}H NMR (400 MHz, CD_3OD) δ 7.21 (s, 2H); 3.87 (s, 6H), 3.81 (s, 3H). 222 $[M + H]^+$. Molecular formula $C_{11}H_{12}N_2O_4$. Yield 75%.

*General procedure for the synthesis of acylguanidines **3-5**.* The aniline hydrochloride **15** or **19a-b** (13.5 mmol, 1 equiv) was dissolved in toluene (800 mL) in the presence of **21** (5.2 g, 14.9 mmol, 1.2 equiv). The reaction mixture was stirred at reflux overnight. The solvent was removed under vacuum and the solid obtained was dissolved in MeOH (35 mL), then a 10% HCl in MeOH solution (30 mL) was added. The mixture was stirred at rt under N_2 overnight to yield the final compounds **3-5**.

4'-Fluoro-N-(2-methyl-5-(3-(3,4,5-trimethoxybenzoyl)guanidino)phenyl)biphenyl-4-carboxamide, HCl (**3**). ^{1}H NMR (400 MHz, DMSO-d_6) δ 12.40 (bs, 1H), 11.52 (bs, 1H), 10.05 (s, 1H), 9.47 (bs, 1H), 9.43 (bs, 1H), 8.95 (bs, 1H), 8.10 (d, *J* = 6.4 Hz, 2H), 7.85-7.80 (m, 4H), 7.60 (s, 1H), 7.55-7.45 (m, 2 H), 7.45-7.24 (m, 4H), 3.92 (s, 6 H), 3.79 (s, 3H), 2.34 (s, 3H).-^{13}C NMR (75 MHz, DMSO, d_6) δ 176.4, 165.6, 164.7, 161.5, 159.9, 153.1, 142.9, 140.8, 137.4, 136.4, 134.8, 133.9, 131.1, 129.8, 129.7, 129.4, 129.2, 127.4,120.2, 120.1, 116.8, 116.5, 106.7, 60.8, 56.4. Mp: 240-245 °C. Elemental analysis for $C_{31}H_{30}ClFN_4O_5$ calcd.: C, 62.78; H, 5.10; Cl, 5.98; F, 3.20; N, 9.45; O, 13.49; found: C, 62.74; H, 5.05; N, 9.47. Yield 82%.

N-(2-Methyl-5-(3-(3,4,5-trimethoxybenzoyl)guanidino)phenyl)biphenyl-4-carboxamide, HCl (***4***)*:* ^{1}H-NMR (400 MHz, DMSO, d_6) δ = 9.18 (bs, 1 H), 9.00 (bs, 1H), 8.06 (bs, 2H), 7.80-7.10 (m, 14H), 3.70 (s, 6H), 3.68 (s, 3H), 2.77 (s, 3 H). ^{13}C NMR (100 MHz, DMSO, d_6) δ 176.0, 168.2, 165.0, 160.0, 156.5, 150.0, 146.3, 139.0, 137.4, 133.1, 131.8, 131.4, 131.0, 128.9, 128.6, 127.1, 127.0, 126.4, 123.5, 121.0, 119.3, 118.5, 116.0, 61.3, 56.0, 34.9. Mp: 250-255 °C. Elemental analysis for $C_{31}H_{31}ClN_4O_5$ calcd.: C, 64.75; H, 5.43; Cl, 6.16; N, 9.74; O, 13.91; found: C, 64.72; H, 5.40; N, 9.79. Yield 92%.

*3,4,5-trimethoxy-N-(N-(4-methyl-3-(4-phenethylbenzamido)phenyl)carbamimidoyl)benzamide, HCl (**5**):* ^{1}H NMR (400 MHz, Methanol-d_4) δ 12.31 (bs, 1H), 11.46 (bs, 1H), 9.90 (bs, 1H), 9.43 (bs, 1H), 8.95 (bs, 1H), 7.92 (s, 1H), 7.75 (d, *J* = 8.0 Hz, 2H), 7.67 (s, 1H), 7.26 (s, 1H),-7.24 (t, *J* = 7.6 Hz, 2H), ~~7.17 (d, *J* = 6.8 Hz, 2H), 7.12 (d, *J* = 8.0 Hz, 2H), 3.82 (s, 9H), 2.96-2.90 (t, *J* = 2.0 Hz, 4H), 2.22 (s, 3H).~~ ^{13}C NMR (101 MHz, Methanol-d_4) δ 176.35, 165.47, 159.01, 146.00, 140.59, 140.31, 136.35, 134.35, 134.78, 132.85, 131.51, 131.23, 131.23, 128.56, 126.01, 127.48, 126.84, 125.71, 120.62, 118.85, 105.54, 60.41, 55.53, 37.21, 36.98, 16.94. ES-MS: 567 $[M + H]^+$, 589 $[M + Na]^+$. Mp: 118-120 °C. Elemental analysis for $C_{33}H_{35}ClN_4O_5$ calcd.: C, 65.72; H, 5.85; Cl, 5.88; N, 9.29; O, 13.26; found: C, 65.75; H, 5.82; N, 9.31. Yield 87%.

2.2. Biology

2.2.1. Drugs. For in vitro experiments, 10 mM stock solutions of **1** and **3**-**6** were prepared in DMSO and stored at -20 °C until use. For oral administration, the compounds were dissolved in a solutol HS15:water mixture (1:20, v/v) and delivered in a volume of 10 mL/kg.

2.2.2. Cell lines and cell cultures. LS180 (human colon adenocarcinoma), HT1080 (human fibrosarcoma) and C3H10T1/2 (Clone 8) (mouse embryonic fibroblast) cells were purchased from ATCC. All cells were routinely cultured in their appropriate growth medium and maintained in a humidified atmosphere with 5% CO_2 at 37 °C. All experiments were performed

starting from frozen cells. Upon thawing, cells were characterized in house by assessing cell morphology, cell growth kinetics curve, and absence of mycoplasma. The human cell lines purchased from accredited biological resource centers (i.e. ATCC) have been originally authenticated and characterized directly by the providers (short tandem repeats profiling). All the experiments have been then performed using cells within 6-8 passages (in the case of human tumor cell lines) or 2 passages (in the case of C3H10T1/2 cells) since thawing from an internal cell bank.

2.2.3. Gli-luciferase reporter assay. Shh-Light II cells, stably incorporating the Gli-luc reporter and the prL-TK *Renilla reniformis* control sequences, were seeded in three 96-well plates at a density of $4 \cdot 10^4$ cells/well. Four days later, they were washed once with PBS (calcium-magnesium free) and incubated for 30 h in 0.5% FBS supplemented medium containing the reference agonist SAG (100 nM), in the presence or in the absence of test compounds (at different concentrations, ranging from 1 to 10000 nM). After incubation, the medium was removed and plates were sealed and frozen at -80 °C. A few days later, plates were thawed and firefly luciferase (expressed under control of a Gli-responsive promoter) and *Renilla* luciferase (expressed under control of a constitutive promoter) were measured by means of the Dual-Glo Luciferase Assay System (Promega, Madison, WI), according to the manufacturer's instructions, using a microplate reader (Victor2, Perkin Elmer). Percentage of inhibition of the SAG-induced Gli-dependent luciferase activity was ultimately calculated with respect to DMSO-treated (control) cells and values were plotted using GraphPad Prism (version 5.02) to determine the $IC_{50} \pm SE$ values. The compounds did not modify significantly the *Renilla* activity at 10 µM.

2.2.4. Alkaline phosphatase (ALP)-based cell differentiation assay. A well-suited ALP assay, enabling to assess the effect of putative Smo inhibitors on differentiation of the mesenchymal pluripotent C3H10T1/2 cells into osteoblasts, was used. C3H10T1/2 cells were seeded into 96-well plates ($3 \cdot 10^3$ cells/well) in complete growth medium. Twenty-four h later, medium was replaced by one supplemented with 2% FBS and containing 0.1 µM SAG as cell differentiation inducer, in the presence or the absence of increasing concentrations of test compounds. Cells were incubated for additional 6 days, then washed once with PBS and lysed by means of a buffer solution (0.1% Triton-X 100, in 150 mM NaCl and 50 mM Tris-HCl, pH 9.5). ALP activity (that is a typical osteoblast marker) was ultimately quantified by adding 10 µL of cell lysates to 50 µL of the CDP-Star chemiluminescence substrate with Sapphire-II Enhancer (molecular probes - Thermo Fisher Scientific), and measuring the resulting chemiluminescence by means of a multiplate reader. Results were expressed, after normalization with respect to protein content of

cell lysates, as percent residual ALP activity compared to cells induced only by SAG. Data were finally plotted and the IC_{50} ± SE values were calculated using GraphPad Prism software.

2.2.5. Proliferation assay. Antiproliferative activity was assessed on two human tumor cell lines: LS180 (colon adenocarcinoma) and HT1080 (fibrosarcoma). Cells were seeded in triplicate in 96-well tissue culture plates in complete medium, and 24 h after seeding they were exposed to increasing concentrations of the test compounds for 72 h. Inhibition of cell proliferation was ultimately assessed by the sulforhodamine B (SRB) assay. The drug potency was evaluated by GraphPad Prism software (version 5.02) and defined as IC_{50} (drug concentration required for 50% inhibition of cell survival) ± SE values.

2.2.6. To evaluate possible off-target effects, **5** has been recently characterized for its activity on a panel of 45 kinases (the Express Diversity Kinase Profile, a 45 kinase activity-based assay utilizing TR-FRET technology, provided by Eurofins Pharma Discovery Services).

2.2.7. Ethics statement. In vivo studies were performed in accordance with the "Directive 2010/63/UE" on the protection of animals used for scientific purposes, made effective in Italy by the Legislative Decree 4 March 2014, n. 26, and applying the principles of 3Rs (namely, replace, reduce, refine). Mice were purchased at Harlan Laboratories (Udine, Italy). All procedures performed on the animals were approved by Animal Welfare Body and authorized by the Italian Ministry of Health, 46/2014-PR. At the end of the treatment period and before necropsy, mice were euthanized by compressed CO_2 gas in cylinder as indicated in the American Veterinary Medical Association Panel on Euthanasia and according to the United Kingdom Co-ordinating Committee on Cancer Research guidelines (UKCCR 1998).

2.2.8. In vivo xenograft models. In vivo experiments on solid tumor models were carried out using 5-6 week-old female athymic nude mice (Harlan Laboratories). Mice were maintained in laminar flow rooms with constant temperature and humidity according to the NIH guidelines. The human tumor xenograft model LS180 (derived from colon carcinoma) was used for antitumor activity study. Exponentially growing tumor cells were s.c. inoculated ($5 \cdot 10^6$/mouse) in the right flank of mice. Groups of eight mice for each experimental group were employed to assess antitumor activity. Drug treatments started 6 days after tumor injection. The compounds were given daily for five days *per* week for 2 weeks. Tumor growth was followed by measurement of tumor diameter with a Vernier caliper. Tumor volume (TV) was calculated using the formula: TV (mm^3) = $[d^2 \cdot D]/2$, where d and D are the shortest and the longest diameter, respectively. The efficacy of the drug treatment was assessed as: TV inhibition percentage (TVI%) in treated versus control mice, calculated as: TVI% = 100 – (mean TV treated/mean TV control · 100). When tumors reached a volume of about 1200 mm^3, mice were

sacrificed by cervical dislocation. To examine the possible toxicity of treatment, body weight was recorded throughout the study.

2.2.9. P-glycoprotein 1 assay. To evaluate the interaction with P-glycoprotein 1 (P-gp), the luminescent P-gp-GloTM ATP-ase Assay (Promega) was used with recombinant human P-gp in a cell membrane fraction. The assay was carried out in quadrupled 96-well plate, according to assay's instruction. Hh inhibitors (10 µM) were tested in comparison to the reference compound verapamil (200 µM). The values were expressed as amount of ATP consumed and fold stimulation.

2.2.10. Caco-2 permeability assay. Caco-2 cell line derived from a human colorectal carcinoma were used. Caco-2 cells (ATCC) were cultured for 20 days in DMEM, media was changed every two or three days. The cells were used between passage numbers 40-60 and seeded on to Millipore Multiscreen Caco-2 plates ($1 \cdot 10^5$ cells/cm^2). On day 20, the monolayers were prepared by rinsing both basolateral and apical surfaces twice with Hank's Balanced Salt Solution (HBSS) at 37 °C. Cells were then incubated with HBSS (atmosphere of 5% CO_2 with a relative humidity of 95% at 37 °C) in both apical and basolateral compartments for 40 min to stabilize physiological parameters. HBSS was then removed from the apical compartment and replaced with test compound solutions for apical to basolateral (A-B) permeability assessment. The fluorescent integrity marker lucifer yellow was also included in the testing solution. Analytical standards were made from testing solutions. The apical compartment inserts were then placed into companion plates containing fresh HBSS. For basolateral to apical (B-A) permeability determination, the experiment was initiated by replacing buffer in the inserts, then placing them in companion plates containing dosing solutions. The companion plate was removed at 120 min, and apical and basolateral samples were diluted for analysis. Test compound permeability was assessed in duplicate. The A-B and B-A permeability coefficient for each compound (Papp) and the influx/efflux ratio (I/E ratio) were calculated. Compounds of known permeability were run as controls on each plate. The Papp A-B and B-A values of test compounds were compared to those of control compounds atenolol and propranolol which have human absorption of approximately 50 and 90%, respectively. The MS/MS analysis for Hh inhibitors resulted in 573.25, 556.27, 538.28, and 566.32 amu for **3**, **4**, **5**, and **6**, respectively, with positive ionization and collision energy of 40 eV for **6** and 30 eV for the other compounds.

2.2.11. CYP_{450} isoforms assay. To investigate the potential drug-drug interaction capabilities of the compounds, the effects of the drugs on CYP1A2, CYP2C9, CYP2C19, CYP2D6, and CYP3A4 activity were examined using P_{450}-GLO-TM assay kits (Promega) according to the manufacturer's instructions. The positive controls (inhibitors of enzyme activity) included α-

naphthoflavone (1 µM) for CYP1A2, sulfaphenazole (10 µM) for CYP2C9, troglitazone (10 µM) for CYP2C19, quinidine (1 µM) for CYP2D6, and ketoconazole (5 µM) for CYP3A4. The compounds were studied using recombinant CYPs, with respect to their capacity to inhibit the formation of luminescent metabolites from CYPs specific luminogenic (proluciferine) substrates. Different concentrations of the compounds (1, 5 and 10 µM), together with reference compounds, positive and negative (blank) controls, were tested in two independent experiments. The assay was performed by incubating a luminogenic CYP substrate with a CYP enzyme and NADPH regeneration system. The luminogenic P_{450}-GloTM substrates are derivatives of beetle luciferin [(4*S*)-4,5-dihydro-2-(6-hydroxybenzothiazolyl)-4-thiazole carboxylic acid], a substrate of firefly luciferase. Light production was evaluated at a luminometer (Glomax-Promega), and values were displayed as Relative Light Unit (RLU). The net CYP-dependent luminescence was calculated by subtracting the average luminescence of the blank from that of the CYP-containing reactions. The percent inhibition of test compound versus the positive control (total activity) was also calculated.

2.2.12. In vitro metabolism in mouse hepatocytes. Cryopreserved mouse hepatocytes were thawed at 37 °C, centrifuged at rt (50*g* for 3 min) and re-suspended at a final concentration of $3 \cdot 10^5$ cells/mL. The viability of the hepatocytes was determined using trypan blue exclusion. Test compounds and reference (7-ethoxy coumarin, 7-ETC) were incubated at 1 µM with a hepatocyte suspension in 24 wells at 37 °C in a CO_2 incubator. Test compounds in buffer (Krebs-Henseleit) and in inactivated hepatocyte suspensions were also included as negative controls. A 50 µL aliquot of the incubation suspension was taken from each well at 0, 5, 15, 30, 60, and 120 min, quenched with methanol or acetonitrile (150 µL), centrifuged at 13000 rpm for 3 min, and analysed by HPLC/MS/MS, using Phenomenex Onyx C18 100 x 4.6 mm chromatographic column and AB-SCIEX API3000 tandem mass spectrometry. The extracts were assayed against a calibration curve ranging from 50 to 1000 ng/mL for all compounds. Run time was approximately 3.5 min. The data were acquired and processed by the data acquisition system Analyst, version 1.5.2. Each time-point was performed in triplicate. The intrinsic clearance (CL_{int}) was calculated using the half-life ($t_{1/2}$) approach. The $t_{1/2}$ and the CL_{int} were determined from the concentration remaining at the different sampling points.

2.2.13. Metabolic stability in mouse plasma. Stability of each compound in murine plasma (200 ng/mL) was investigated at 37 °C. Compounds were tested in triplicate and the samples were collected at 0, 15, 30, 45, 60, and 120 min. The same compounds in deproteinized plasma were used as metabolic stability controls. Collected samples were deproteinized by adding acetonitrile

and analyzed by HPLC/MS/MS in the same conditions described for the in vitro metabolism in mouse hepatocytes.

2.2.14. Pharmacokinetic study. CD1 male mice were treated orally with a single dose of the compounds at 200 mg/kg using 20% solutol HS 15 in water. Blood samples were collected at 0.25, 0.5, 1, 2, 4, 6, and 24 h post treatment from 4 animals *per* time point. Levels of the compounds were determined in plasma by quantitative HPLC-MS/MS having a method range from 50 to 1000 ng/mL for all compounds. The PK parameters C_{max} (maximum plasma concentration), T_{max} (time of maximum plasma concentration), C_{last} (last quantifiable concentration), T_{last} (time of last quantifiable plasma concentration), AUC_{last} (area under the concentration versus time curve from 0 to T_{last}), AUC_{INF} (area under the concentration versus time curve from 0 to infinity), $t_{1/2}$ (terminal half-life), CL/F (apparent systemic clearance), and Vz/F (apparent terminal volume of distribution), were derived from the analyte plasma concentration versus time data according to a model-independent approach for sparse data sampling by using Phoenix WinNonlin software, version 6.3 (Pharsight, Certara, Princeton, NJ).

Statistical analysis. Data are expressed as the mean ± SD or S.E.M. Statistical analysis was performed using Mann-Whitney's test. A P-value of ≤ 0.05 was considered statistically significant.

3. Results

3.1. Medium scale synthesis of the compounds

A medium-scale (5-7 g), more sustainable synthesis of the acylthiourea (**6**) and acylguanidine (**3-5**) derivatives was developed for the first time to allow for a possible large scale-up and for the in vivo studies. A convergent approach seemed to be the most valuable for this purpose, coupling a proper functionalized aniline (**A**) with acyl chloride (**20**) or acyl cyanamide (**21**) to obtain acylthiourea and acylguanidine derivatives, respectively (Figure 3). Moreover, a classical amide synthesis, using a properly functionalized acyl chloride (**B**) and the nitro aniline **12,** was planned for the synthesis of aniline derivative **A**.

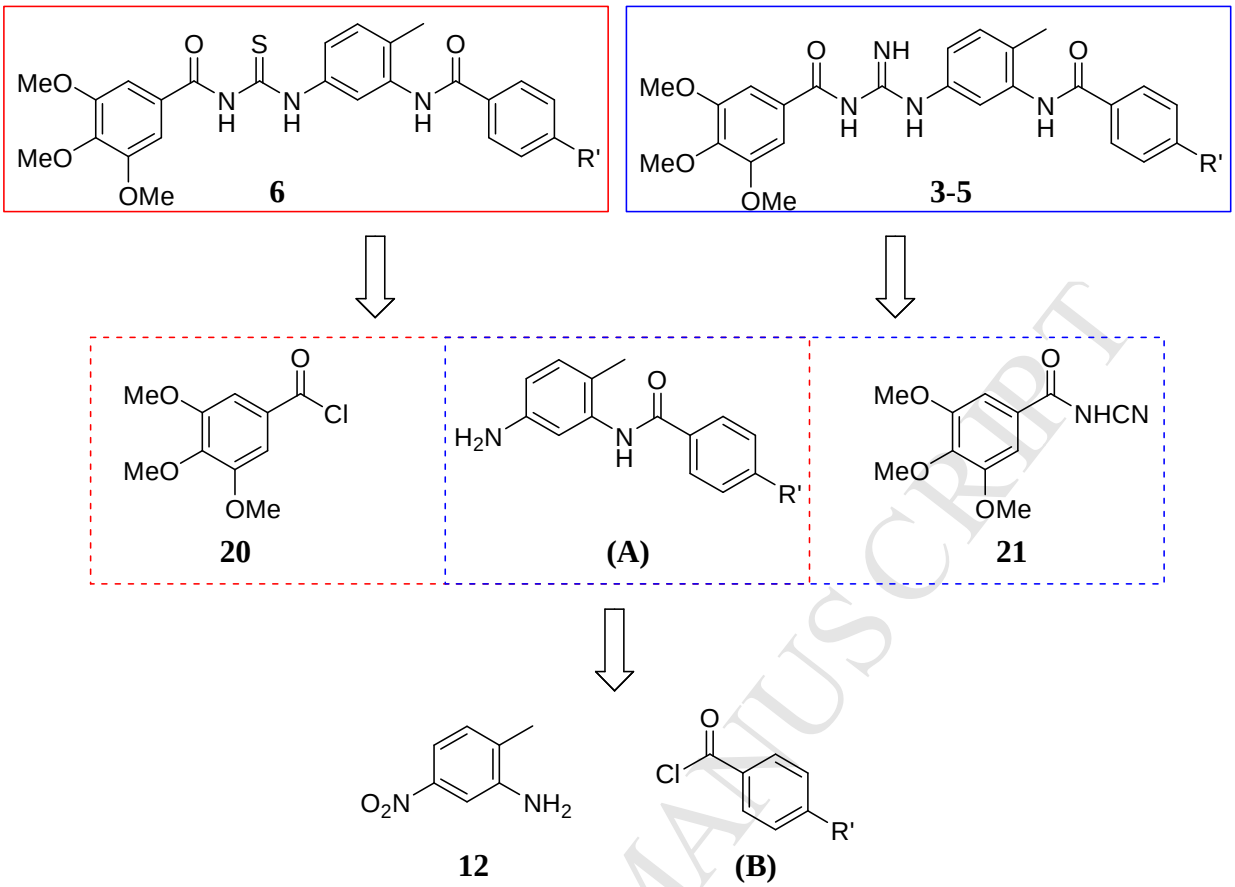

Figure 3. Retrosynthetic approach for the synthesis of the studied acylguanidines and acylthioureas.

The acyl chlorides **(B)** required for the synthesis of **3**, **4**, and **6** are commercially available, while the preparation of a suitable chloride was required for **5**. Previously, we have applied a Wittig reaction to obtain a small-scale amount (about 100 mg) of **10** [17]. However, while this reaction was a good opportunity for the early hit identification/optimization steps, the same protocol was not suitable for the large-scale synthesis of this compound as the reaction lacked for poor atom economy (*i.e.* production of 1 equivalent of triphenylphosphine oxide as by-product, and use of dangerous bases such as BuLi in overstoichiometric amounts), long reaction times, change in reaction temperature (from -78 °C to rt), and low yield.

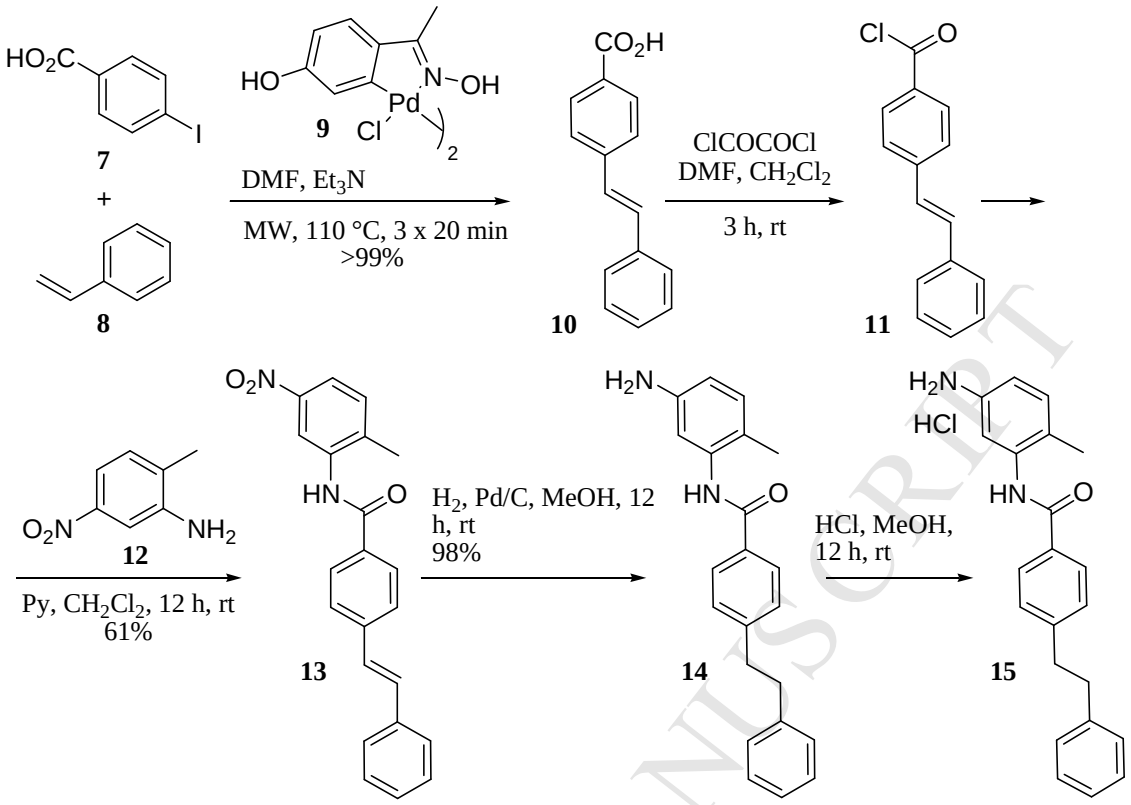

Scheme 1. Synthesis of **15**.

For these reasons, the use of a more sustainable catalytic protocol involving an Heck coupling between 4-iodobenzoic acid **7** and styrene **8** in the presence of freshly prepared Pd catalyst **9** [26], in DMF and Et_3N taking advantage from MW irradiation at 110 °C for 20 min, was investigated (Scheme 1). The irradiation was repeated for three times. The conversion into **10** was finally quantitative and the product was directly crystallized from H_2O. To avoid side reactions and by-products during the synthesis of **11**, a purification of **10** by flash chromatography demonstrated to be a mandatory step for removing Pd traces responsible, in medium-scale, for aniline **12** demethylation during the coupling. A summary of the advantages in terms of sustainability of the developed Heck coupling is reported in Table 2 [27].

The acid **10** was transformed into its acyl chloride derivative (**11**) by treatment with oxalyl chloride in the presence of a catalytic amount of DMF and directly reacted with **12** in the presence of pyridine as the base. The nitro derivative **13** was obtained in 61% yield after a simple acid-base extraction during the work-up. In the small-scale protocol already reported [16], a MW-assisted hydrogenation reaction using ammonium formiate as the hydrogen source in the presence of Pd/C was applied to obtain **14**. Nevertheless, this protocol failed in medium-scale preparation because of several security issues: i) the reaction mixture is completely heterogeneous as none of the reactants, reagents, and the catalyst (**13**, HCO_2NH_4 and Pd/C,

respectively) are soluble in MeOH; ii) the reaction is really exothermic, and iii) working on a 500 mg scale, an explosion occurs after 30 s MW irradiation. For these reasons, we finally decided to simultaneously reduce both the nitro group and the double bond by treatment of **7** with 10% Pd/C in MeOH directly using the more atom economic H_2 atmosphere (1 atm) at rt overnight. The expected product, obtained in quantitative yield, was directly transformed into the hydrochloric salt **15** for the preparation of the corresponding acyl guanidine.

A similar approach, starting from commercially available biphenyl-4-carbonyl chloride (**16a**) and 4'-fluorobiphenyl-4-carbonyl chloride (**16b**), was successfully applied to the synthesis of anilines **18a-b** and their hydrochloric salts **19a-b**, as reported in Scheme 2.

Table 2. Higher sustainability of the Heck coupling in comparison to a Wittig reaction for the synthesis of the studied compounds.

Parameters	**Wittig reaction**	**Heck coupling**
Solvent	THF (20 mL for 2 mmol SM[a] or 180 mL for 12 mmol SM)	DMF (15 mL for 12 mmol SM)
Additives	*BuLi (3.5 equiv = 448 mg for 2 mmol SM or 2.6 g for 12 mmol SM)*	*Et_3N (1.4 equiv = 1.7 g for 12 mmol SM)* *Pd cat. (0.01 equiv = 78 mg for 12 mmol SM)*
By-products	$POPh_3$ (1 equiv = 556 mg for 2 mmol SM or 3.4 g for 12 mmol SM) LiBr (1 equiv = 166 mg for 2 mmol SM or 996 mg for 12 mmol SM)	Et_3NHI (1 equiv = 2.7 g for 12 mmol)
Temperature	*-78 °C (Cryostate) and rt*	*110 °C (MW)*
Time	1 h + 12 h	1.5 h
Flammable reagents	*BuLi (+++), THF (+)*	*DMF (+)*
Purification	Extraction (AcOEt), column	Precipitation (1N HCl), column
Yield	*70%*	*>99%*

[a]SM = Starting material.

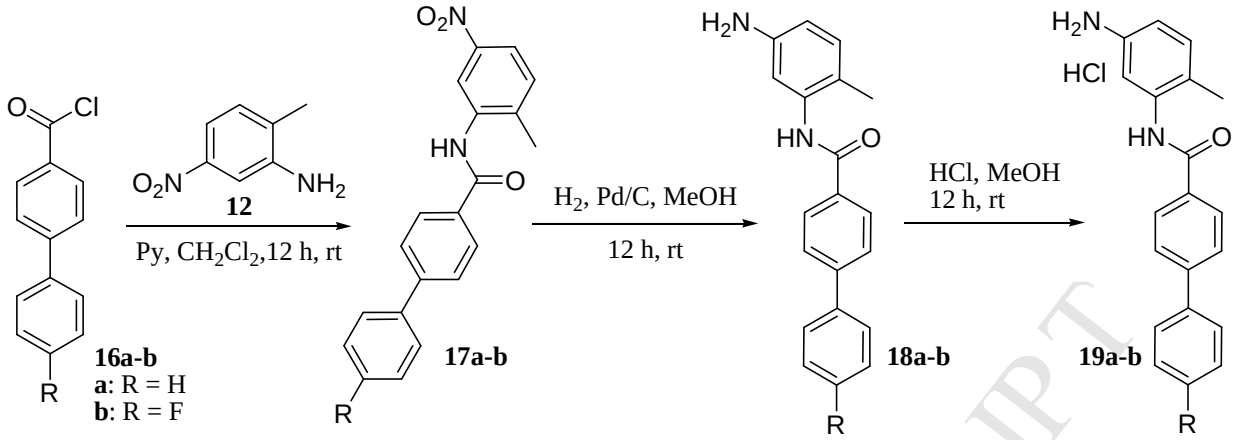

Scheme 2. Synthesis of **19a-b**.

The final thiourea **6** was obtained by treatment of **18b** with ammonium thiocyanate and trimethoxy benzoyl chloride **20** in acetone at reflux for 3 h. A white solid (86% yield) resulted after crystallization (Scheme 3).

Aniline hydrochlorides **15** and **19a-b** reacted with acylcyanamide **21** in toluene at reflux to give the acylguanidines that were finally transformed into their hydrochloric acid salts **3-5**. All these derivatives were synthesized in 5 to 7 g scale with purity >97%.

The protocol developed demonstrates to be effective for the large-scale synthesis of both acylthiourea and acylguanidine compounds, avoiding the risk of using procedures that are known to lack for sustainability and safety issues.

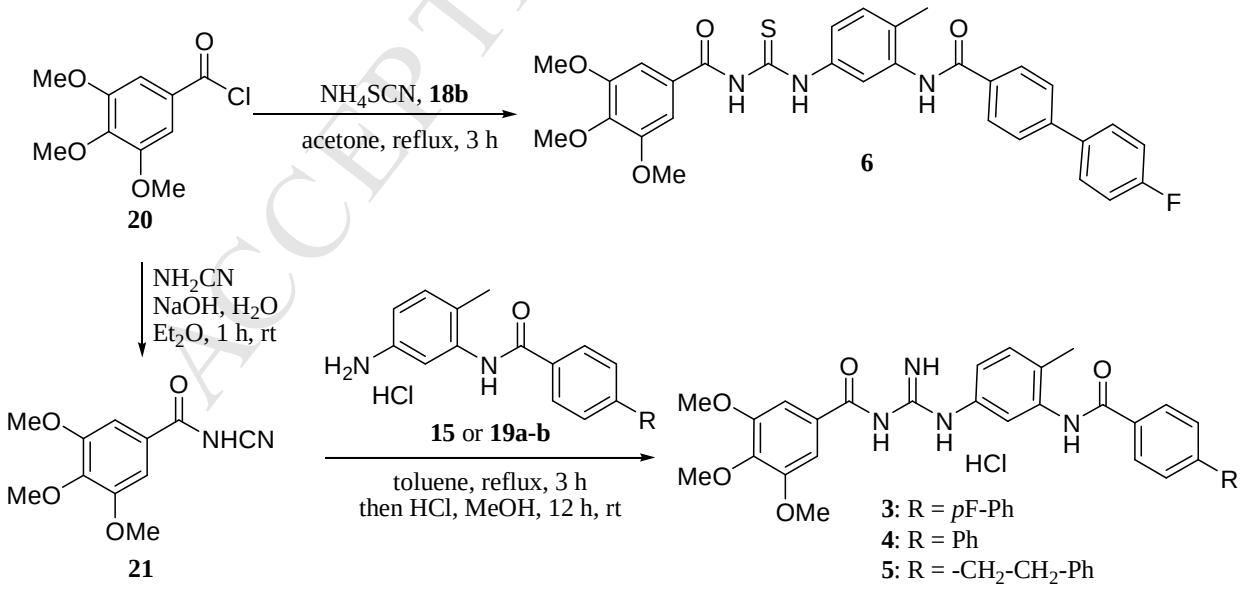

Scheme 3. Synthesis of the final compounds.

3.2. In vitro pharmacology

In vitro treatment with the compounds resulted in Hh signaling inhibition and decreased viability of colon cancer and fibrosarcoma cell lines.

To assess whether **3-6** could inhibit the Hh signaling pathway, a Gli-luciferase gene reporter assay and a cell differentiation assay were performed including **1** as positive control. Although a similar evaluation of **3-5** were previously reported by us [16, 17, 21], the Gli-luc and the alkaline phosphatase-based assays (see below) were repeated to collect homogeneous biological data, including those of the new compound **6**.

The Shh-light II cell line, a clonal NIH-3T3 cell line expressing Gli-responsive firefly luciferase and constitutive *Renilla* luciferase reporters, was stimulated for 30 h with 0.1 µM SAG in the presence or absence of test compounds at various concentrations (from 0.001 to 10 µM). Overall, the compounds inhibited the Gli-responsive reporter activity induced by SAG in a dose-dependent manner, with IC_{50} values ranging from 20 to 100 nM (Table 3, Figure 4).

Compound **5** resulted the most active and its inhibitory activity (IC_{50} = 0.02 µM) was also stronger than that of **1** (IC_{50} = 0.05 µM).

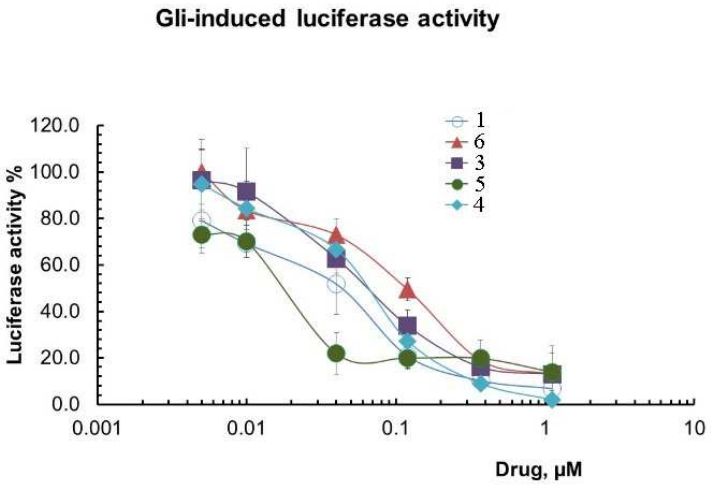

Figure 4. Inhibition of SAG-induced Gli-dependent luciferase activity in Shh-Light II cells by compounds **3-6** in comparison to **1** used as reference compound. Inhibition curves were generated using increasing concentrations of compounds in the presence of SAG (0.1 µM). The values are expressed as a percentage of the residual luciferase activity, and are the means ± S.E. of triplicates. The data shown are representative of 2 independent experiments.

To confirm the data, a second orthogonal assay was performed on the mesenchymal pluripotent C3H10T1/2 cells that, once induced with Hh ligands, differentiate into ALP-positive osteoblasts [28, 29]. Exposure of these cells to the compounds for 6 days suppressed, in a dose-dependent

manner, ALP activity evoked by SAG (Table 3, Figure 5). As in the previous reporter assays, **5** (IC_{50} = 0.04 µM) was shown to be the most active compound.

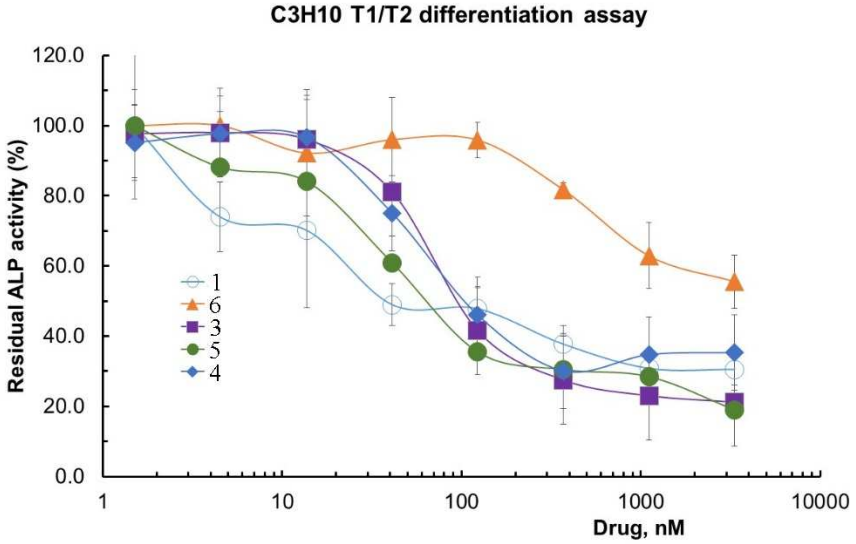

Figure 5. Inhibition of ALP activity in SAG-induced C3H10T1/2 cells by the compounds in comparison to **1** used as reference compound. Inhibition curves were generated using increasing concentrations of compounds in the presence of SAG (0.1 µM). The values are expressed as a percentage of the maximal response induced by SAG, and are the means ± S.E. of triplicates. The data shown are representative of two independent experiments.

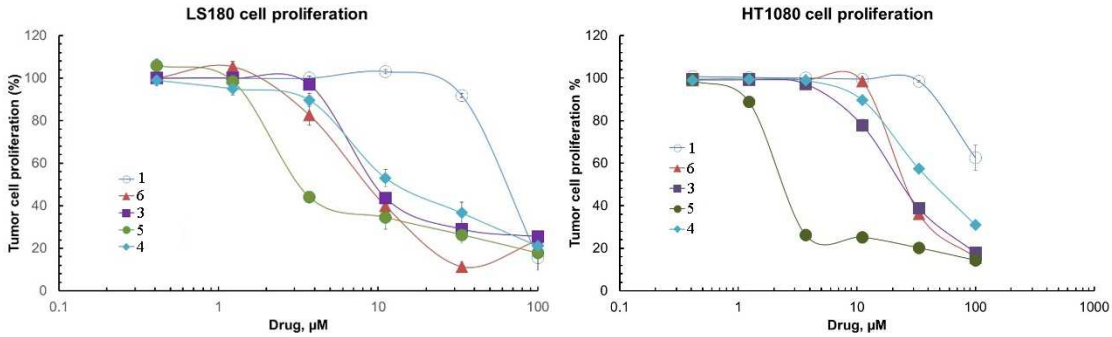

Figure 6. Inhibition of LS180 (left) and HT1080 (right) cell proliferation upon a 72 h treatment with the compounds in comparison to **1** used as reference compound. Results, expressed as tumor cell proliferation percent with respect to DMSO-treated (control) cells, are the means ± S.E. of triplicates.

In order to test the ability of the compounds to inhibit growth and viability of tumor cells, LS180 human colon carcinoma and HT1080 human fibrosarcoma cell lines were used in SRB assay, after 72 h incubation (Figure 6). All the compounds potently inhibited cell proliferation of both cell lines, in a dose-dependent manner. Anti-proliferative activity was 5-18 and 3-50 fold better than that of **1** against LS180 and HT1080 cells, respectively. Consistently with previous data, **5**

resulted the most active compound and showed a similar activity against both cell lines (IC_{50} values of 2.5 and 2.0 μM, respectively). These activities were at least three-fold higher than that of the other compounds, including **1**.

Overall in vitro pharmacology data reported in Table 3 confirm that the compounds significantly inhibited Hh signaling pathway and tumor cell proliferation with **5** being the most active compound.

Moreover, evaluation of **5** on a panel of 45 kinases resulted in percent inhibition of control values lower than 15% in all cases, thus demonstrating that **5** did not affect significantly the activity of these targets (no off-target effects).

Table 3. Summary of comparative effects of the compounds and the reference Smo inhibitor **1** in different cell-based assays.[a]

Compound	Tumor Cell Viability[b]		Luciferase activity (Shh-Light II cells)[c]	ALP activity (C3H10T1/2 cells)[d]
	LS180	HT1080		
1	45 ± 5	>100	0.05 ± 0.01	0.05 ± 0.01
3	8.1 ± 1.0	20 ± 1	0.05 ± 0.01	0.07 ± 0.01
4	9.7 ± 1.2	29 ± 1	0.07 ± 0.01	0.06 ± 0.01
5	2.5 ± 0.3	2.0 ± 0.5	0.02 ± 0.01	0.04 ± 0.01
6	7.5 ± 1.1	27 ± 1	0.10 ± 0.01	0.67 ± 0.02

[a]Values are reported as IC_{50} ± SE (expressed in micromolar concentrations) and were calculated as mean of at least two experiments.

[b]Inhibition of tumor cells proliferation, by SRB assay; upon a 72 h treatment.

[c]Inhibition of the Gli-luciferase reporter activity in Shh-Light II cells after treatment with various concentrations of the compounds for 30 h. The firefly luciferase activity (expressed under control of a Gli-responsive promoter) and the Renilla luciferase activity (expressed under control of a constitutive promoter) were measured using the Dual-Glo Luciferase Assay System. Percentage of inhibition of the SAG-induced Gli-dependent luciferase activity was ultimately calculated with respect to DMSO-treated (control) cells.

[d]Inhibition of ALP activity induced by SAG (0.1 μM) in C3H10T1/2 cells. Cells were treated with various concentrations of the compounds for 6 days.

3.3. In vivo activity

The oral administration of **5** inhibited the tumor growth of a colon carcinoma xenograft cancer in nude mice. The LS180 colon cancer xenograft model was used to explore the effect of the compounds on Hh-dependent tumors in vivo. LS180 tumor cells secrete Hh ligands, thus leading

to enhanced Gli1 transcription. Mice bearing established LS180 tumors were administered by oral route with 200 mg/kg of test compounds (**3**-**5**) daily (5 days/week) for 2 weeks and tumor growth was monitored. Only **5** significantly inhibited tumor growth by 48% compared to vehicle-treated controls (P<0.01, Mann-Whitney's test) (Figure 7). No toxicity in terms of body weight loss was observed.

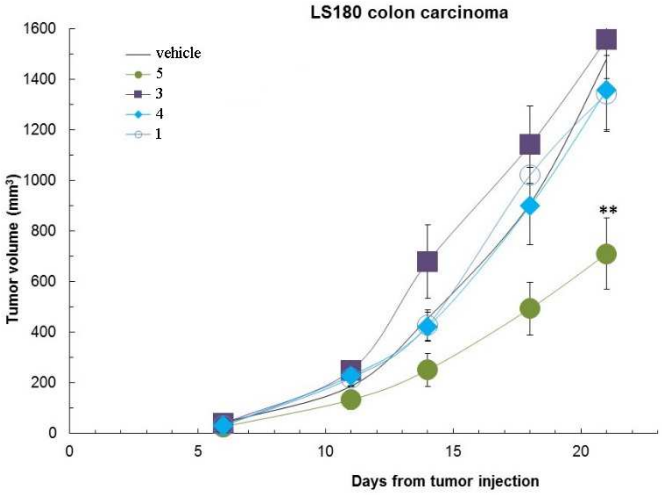

Figure 7. In vivo tumor growth inhibition induced by the compounds in comparison to **1** used as reference compound. LS180 colon cancer cells were injected in nude mice and 6 days after tumor implantation, the test compounds were delivered by oral route. Tumor lesions were measured by Vernier caliper.

3.4. In vitro ADME parameters and pharmacokinetics of the compounds orally administered in mice

3.4.1. P-glycoprotein 1 assay. A linear standard curve of ATP ranging from 37.5 to 300 nM was built to calculate P-gp ATPase activity through ATP consumption. Compound **3** and **6** showed a low effect on P-gp ATPase activity (fold induction of 3.0 and 2.3, respectively, Table 4), while **4** appeared to be a potential substrate of P-gp (fold induction of 4.8). Compound **5** did not have any interaction with the P-gp. Verapamil, used as reference compound, induced a 8.5-fold stimulation of P-gp ATPase activity.

Table 4. In vitro effect of the compounds on P-gp.

Compd	ATP[a]	Fold stimulation[b]
Basal activity	13	
3	30	2.3
4	63	4.8
5	18	1.4
6	39	3.0
verapamil	111	8.5

[a]P-gp ATPase activity was expressed as picomoles of ATP consumed *per* µg P-gp *per* minute and was calculated converting RLU value to ATP concentrations by a standard curve of ATP.
[b]Fold stimulation was the ratio of ATP over basal value.

3.4.2. Caco-2 Permeability assay. Influx/Efflux (I/E) ratio of the compounds in Caco-2 colon cancer cells is shown in Table 5. Compound **6** was not detectable in receiver compartment with a high value of starting concentration. Compounds **3** and **5** had an I/E ratio ~1, suggesting that they could not affect the human absorption. Compound **4** showed a low recovery that could be indicative of non-specific binding issues. However, its I/E ratio <2 suggested a low potential to be a P-gp substrate. Atenolol (paracellular transport) and propranolol (passive transcellular transport) with known human absorption of 50% and 90% respectively, as well as talinolol (a P-gp substrate), were used as reference compounds to confirm that tumor cells were expressing functional influx/efflux proteins.

Table 5. Evaluation of bi-directional permeability of Hh inhibitors.

Compd	P_{app} A-B[a]	% recovery	P_{app} B-A[a]	% recovery	I/E ratio[b]
3	0.366±0.044	33.0	0.370±0.006	30.6	1.01
4	0.428±0.063	16.5	0.651±0.016	31.9	1.52
5	0.701±0.166	41.1	0.737±0.189	44.6	1.05
6		65.4		42.9	
atenolol	0.316±0.045	94.7	0.721±0.018	102	2.28
propranolol	30.9±0.7	70.0	21.1±2.3	89.0	0.68
talinolol	0.162±0.020	94.8	12.6±0.3	88.6	78.2

[a]Values are the mean ± SD of two replicates, expressed in $10^{-6}\cdot cm\cdot s^{-1}$. Atenolol (paracellular transport), propranolol (passive transcellular transport), and talinolol (P-gp substrate) were used as reference compounds.

[b]I/E ratio = (mean P_{app} B-A/mean P_{app} A-B).

3.4.3. CYP_{450} isoform assay. Except **6**, all the compounds interfered (as competitive substrates or inhibitors) with the activity of CYP1A2 and CYP3A4, sometimes in a concentration-dependent manner. All the compounds interfered with the activity of CYP2C9 and CYP2C19 without a clear dependency on their concentration. Finally, none of the compounds interfered significantly with CYP2D6. Interfering effects (%) are shown in Table 6 as mean (±S.E.M) of triplicate assays.

Table 6. Interfering effects (% ± S.E.M.) of the studied and reference compounds on cytochrome CYP_{450} enzymes.[a]

CYP	**1A2**			**3A4**			**2C9**		
(µM)	1	5	10	1	5	10	1	5	10
3	46±1	58±2	59±2	52±9	78±5	-82±8	63±1	76±1	79±2
4	49±1	64±2	64±2	38±8	76±3	-87±3	43±3	71±0	74±3
5	29±2	43±1	40±2	76±3	89±2	-92±2	68±1	81±0	83±1
6	2±3	5±4	1±2	4±11	7±15	15±21	63±1	69±1	71±0
CYP	**2C19**			**2D6**					
(µM)	1	5	10	1	5	10			
3	59±2	76±0	76±1	20±4	25±5	21±5			
4	57±1	79±0	81±1	19±4	29±2	23±5			
5	67±1	81±1	83±1	15±5	12±4	11±3			
6	25±2	33±1	27±2	18±9	1±8	6±5			

[a]Reference compounds. CYP1A2: α-naphthoflavone (1 µM, 98%); CYP3A4: ketoconazole (5 µM, 96%); CYP2C9: sulfaphenazole (10 µM, 98%); CYP2C19: troglitazone (10 µM, 84%); CYP2D6: quinidine (1 µM, 91%).

3.4.4. In vitro metabolism in mouse hepatocytes. Compound **3** and **4** showed chemical instability, so the CL_{int} could not be calculated. By contrast, **5** had a CL_{int} of 756 mL/min/kg with a $t_{1/2}$ value of about 8 min (Table 7). The reference compound, 7-ETC, revealed a $t_{1/2}$ of about 5 min and a CL_{int} corresponding to 1260 mL/min/kg, as described in the literature.

Table 7. In vitro mouse hepatocytes metabolism.

Compound[a]	$t_{1/2}$ (min)	CL_{int} (µL/min/10^6 cells)	CL_{int} (mL/min/kg)
5	8.07	286	756
7-ETC	4.84	477	1260

[a]The compounds and 7-ETC (reference compound) were incubated at the concentration of 1 µM with mouse hepatocytes. ND = not determined.

3.4.5. Metabolic stability in murine plasma. The compounds showed different metabolic stability in murine plasma at 37 °C up to 120 min. Compound **6** was highly metabolized, while **3** and **5** were moderately metabolized. Conversely, **4** was metabolically stable (Figure 8). When incubated in deproteinized plasma, the recovery of **4** was about 83%, the same value observed after incubation with mouse plasma, thus indicating chemical instability instead of metabolism. All the other compounds were stable when incubated over 120 min in deproteinized plasma at 37 °C.

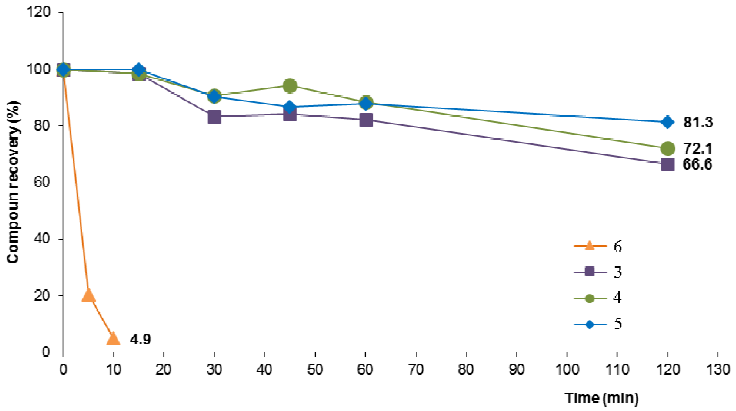

Figure 8. Percent values of **3-6** recovered after a 120 min incubation at 37 °C in mouse plasma. Noteworthy, when incubated in deproteinized plasma over 120 min at 37 °C, the recovery of **4** was about 83%, the same observed after incubation with fresh mouse plasma. For Vismodegib plasma stability see Ref. 30.

3.4.6. In vivo oral pharmacokinetics in mouse. The PK profile in healthy mice was determined after a single dose of 200 mg/kg of each compound administered by oral route. Compound **6** was sporadically quantified in mouse plasma (2 out the 32 samples collected). The remaining compounds were detected in all the plasma samples collected up to last collection time (24 h). Compounds **3** and **5** showed multiple peaks in plasma profiles, the highest of which occurred at

1.0 and 4.0 h, respectively. Conversely, **4** was rapidly absorbed and showed a C_{max} of about 30 µg/mL 2 h after dosing. Subsequently, its plasma concentration declined according to a mono-exponential profile (Figure 9).

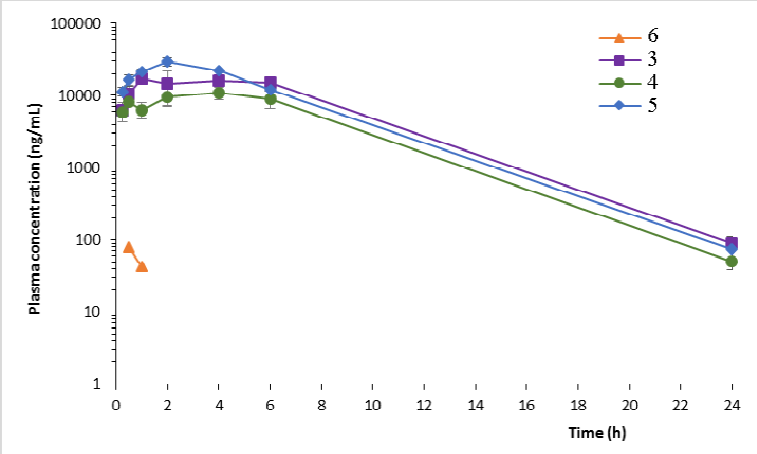

Figure 9. Mean (± S.E.M) plasma concentration versus time profiles (log-linear scale) of **3-6** in CD-1 male nude mice receiving a 200 mg/kg single oral dose of each test compound. For Vismodegib *in vivo* stability see Ref. 30.

All compounds were cleared from plasma with a $t_{1/2}$ of about 2.5 h. Compounds **3** and **4** showed similar CL/F (893 and 843 mL/h/kg), lower than that of **5** (1460 mL/h/kg). Accordingly, the systemic exposur of **3** and **4** was higher than that of **5**. PK parameters are summarized in Table 8.

Table 8. Pharmacokinetic parameters of the studied compounds determined after a 200 mg/kg single dose to CD-1 male nude mice.[a]

Compd	C_{max}[b]	T_{max}	C_{last}	T_{last}	AUC_{last}[b]	AUC_{INF}	$t_{1/2}$	CL/F	Vz/F
3	17.3±2.3	1	90.7	24	223±31	223970	2.6	893	3323
4	29.6±3.9	2	74.2	24	237±17	237226	2.4	843	2963
5	11.0±2.2	4	50.7	24	137±23	136943	2.5	1460	5280

[a]Abbreviations used. C_{max}: maximum plasma concentration, in µg/mL; T_{max}: time of C_{max}, in h; C_{last}: last quantifiable concentration, in µg/mL; T_{last}: time of C_{last}, in h; AUC_{last}: area under the concentration *versus* time curve from 0 to T_{last}, in µg·h/mL; AUC_{INF}: area under the concentration *versus* time curve from 0 to infinity, in µg·h/mL; $t_{1/2}$: terminal half-life, in h; CL/F: apparent systemic clearance, in mL/h/kg; Vz/F: apparent terminal volume of distribution, in mL/kg.

[b]Mean ± S.E.M.

4. Discussion

A preliminary in vitro investigation on acylthiourea and acylguanidine derivatives showed their ability to impair Smo activity at nanomolar concentrations also toward Smo mutants resistant to already known antagonists [17]. These results prompted us to carry out a preliminary non-clinical characterization of their in vitro ADME and in vivo pharmacokinetic profile, and to eventually prioritize the best compound eligible for further clinical development.

For this purpose, the medium-scale synthesis of **3**-**6** was for the first time approached, taking also into account sustainable and safety issues for a future scale-up of the overall process. All the compounds were obtained in large quantity (5-7 g) with very high purity, using the more sustainable protocols developed so far for the synthesis of this family of compounds.

In addition, we further support the hypothesis that these compounds, in particular **5**, selectively suppressed the Hh signalling pathway activity by potentially targeting the critical component Smo and consequently inhibiting the Hh-dependent cancer growth.

In vitro ADME properties and in vivo pharmacokinetic studies in mouse, after a single oral dose, were investigated. In vitro studies suggested that none of the compounds were potential P-pg substrates. However, they underwent extra-hepatic (**6** only) or moderate hepatic metabolism. Except **6**, the compounds were potential substrates and/or inhibitors of CYP1A1 and CYP3A4, all interfered with the activity of CYP2C9 and CYP2C19, and none of them with the activity of CYP2D6. The in vitro ADME profiles were in good agreement with the in vivo pharmacokinetic profiles observed in nude mice after a single oral 200 mg/kg dose of each compound. Compound **6** showed an extremely low bioavailability, probably due to its extensive extra-hepatic metabolism, rather than to an incomplete absorption. Compounds **3**-**5** showed similar plasma profiles in nude mice having a terminal half-life of about 2.5 h. However, **5** had a lower systemic exposure compared to **3** and **4**, possibly because of its higher hepatic metabolism and/or larger volume of distribution (assuming a similar bioavailability as argued by in vitro tests). Considering that **5** effectively inhibited in vivo tumor growth of colorectal cancer LS180, thus indicating that such a compound is distributed outside the systemic circulation to reach the target tissues, we hypothesize that a large volume of distribution rather than a high clearance could be responsible for its low systemic exposure.

Moreover, **5** effectively inhibited tumor growth without affecting body weight, and significantly suppressed the Hh signalling pathway in tumor lesions.

In the present study, we identified **5** as a strong inhibitor of the Hh pathway activity by targeting Smo. Using a colon cancer model overexpressing the Hh ligand, we also demonstrated that the same compound significantly impaired Hh-dependent tumor growth by inhibiting Hh pathway activity. The ability of this compound to inhibit Smo activity also in mutant cells resistant to **1** and other known Smo inhibitors, could give support to the future usage of **5** for treating cancers driven by aberrant Hh pathway. Given that **5** showed a good PK and metabolic profile, it could be further investigated (alone or in combination with other treatment strategies) for a clinical efficacy on patients with tumors dependent on the Hh pathway disregulation.

5. Disclosure of potential conflicts of interest

LV, FMM, MAS, SP, FrM, CT, RDS, and GG are ALFASIGMA employees. The remaining authors disclosed no conflicts of interest. All authors have approved the final form of this article.

6. Author contribution

EP planned the large scale synthesis. EC and EP synthesized the compounds, LV, FMM, RDS coordinated the in vitro and in vivo studies. LV, FaM, MAS, EP analyzed data and wrote the manuscript. MAS, SP, FrM and CT performed PK studies. GG coordinated the project.

7. Acknowledgements

The authors would like to thank Giuseppe Roscilli, Emanuele Marra, Fabiana Fosca Ferrara, and Luigi Aurisicchio of Takis-Biotech s.r.l. (Castel Romano, Rome, Italy) for their support for in vitro and in vivo studies. The Italian Ministry of Education, University, and Research (MIUR) is also acknowledged for a Grant as Dipartimento di Eccellenza 2018-2022.

8. Appendix A. Supplementary data

Supplementary data related to this article can be found at

9. References

[1] N.S. Chari, T.J. McDonnell, The sonic hedgehog signaling network in development and neoplasia, Adv. Anat. Pathol. 14 (2007) 344-352. DOI: 10.1097/PAP.0b013e3180ca8a1d.

[2] J. Briscoe, P.P. Therond, The mechanisms of Hedgehog signaling and its roles in development and disease, Nat. Rev. Mol. Cell Biol. 14 (2013) 416-429. DOI: 10.1038/nrm3598.

[3] S.J. Scales, F.J. de Sauvage, Mechanisms of Hedgehog pathway activation in cancer and implications for therapy, Trends Pharmacol. Sci. 30 (2009) 303-312. DOI: 10.1016/j.tips.2009.03.007.

[4] S. Teglund, R. Toftgard, Hedgehog beyond medulloblastoma and basal cell carcinoma, Biochim. Biophys. Acta 1805 (2010) 181-208. DOI: 10.1016/j.bbcan.2010.01.003.

[5] Y. Bilir, E. Gokce, B. Ozturk, F.A. Deresoy, R. Yuksekkaya, E. Yaman, Metastatic basal cell carcinoma accompanying Gorlin syndrome, Case Rep. Oncol. Med. 2014 (2014) 362932. DOI: 10.1155/2014/362932.

[6] M. Guha, Hedgehog inhibitor gets landmark skin cancer approval, but questions remain for wider potential, Nat. Rev. Drug Discov. 11 (2012) 257-258. DOI: 10.1038/nrd3714.

[7] T.K. Rimkus, R.L. Carpenter, S. Qasem, M. Chan, H.-W. Lo, Targeting the Sonic Hedgehog signaling pathway: review of Smoothened and GLI inhibitors, Cancers 8 (2016) 22. DOI: 10.3390/cancers8020022.

[8] https://www.accessdata.fda.gov/drugsatfda_docs/label/2012/203388lbl.pdf (accessed 16 July 2018).

[9] https://www.accessdata.fda.gov/drugsatfda_docs/label/2015/205266s000lbl.pdf (accessed 16 July 2018).

[10] A. Sekulic, M.R. Migden, A.E. Oro, L. Dirix, K.D. Lewis, J.D. Hainsworth, J.A. Solomon, S. Yoo, S.T. Arron, P.A. Friedlander, E. Marmur, C.M. Rudin, A.L. Chang, J.A. Low, H.M. Mackey, R.L. Yauch, R.A. Graham, J.C. Reddy, A. Hauschild, Efficacy and safety of vismodegib in advanced basal-cell carcinoma. N. Engl. J. Med. 366 (2012) 2171-2179. DOI: 10.1056/NEJMoa1113713.

[11] https://clinicaltrials.gov (accessed 16 July 2018).

[12] D. Amakye, Z. Jagani, M. Dorsch, Unraveling the therapeutic potential of the Hedgehog pathway in cancer. Nat. Med. 19 (2013) 1410-1422. DOI: 10.1038/nm.3389.

[13] C. Danial, K.Y. Sarin, A.E. Oro, A.L. Chang, An investigator-initiated openl trial of sonidegib in advanced basal cell carcinoma patients resistant to vismodegib, Clin. Cancer Res. 22 (2016) 1325-1329. doi: 10.1158/1078-0432.CCR-15-1588.

[14] T.W. Ridky, G. Cotsarelis, Vismodegib resistance in basal cell carcinoma: not a smooth fit, Cancer Cell 7 (2015) 315-316. doi: 10.1016/j.ccell.2015.02.009.

[15] S.X. Atwood, K.Y. Sarin, R.J. Whitson, J.R. Li, G. Kim, M. Rezaee, M.S. Ally, J. Kim, C. Yao, A.L. Chang, A.E. Oro, J.Y. Tang, Smoothened variants explain the majority of drug resistance in basal cell carcinoma, Cancer Cell 27 (2015) 342-353. doi: 10.1016/j.ccell.2015.02.002.

[16] A. Solinas, H. Faure, H. Roudaut, E. Traiffort, A. Schoenfelder, A. Mann, F. Manetti, M. Taddei, M. Ruat, Acylthiourea, acylurea, and acylguanidine derivatives with potent Hedgehog inhibiting activity, J. Med. Chem. 55 (2012) 1559-1571. DOI: 10.1021/jm2013369.

[17] L. Hoch, H. Faure, H. Roudaut, A. Schoenfelder, A. Mann, N. Girard, L. Bihannic, O. Ayrault, E. Petricci, M. Taddei, D. Rognan, M. Ruat, MRT-92 inhibits Hedgehog signaling by blocking overlapping binding sites in the transmembrane domain of the Smoothened receptor, FASEB J. 29 (2015) 1817-1829. DOI: 10.1096/fj.14-267849.

[18] A. Chiarenza, F. Manetti, E. Petricci, M. Ruat, A. Naldini, M. Taddei, F. Carraro, Novel acylguanidine derivatives targeting Smoothened induce antiproliferative and pro-apoptotic effects in chronic myeloid leukemia cells, PLoS One 11 (2016) e0149919. DOI: 10.1371/journal.pone.0149919.

[19] S. Pietrobono, S. Santini, S. Gagliardi, F. Dapporto, D. Colecchia, M. Chiariello, C. Leone, M. Valoti, F. Manetti, E. Petricci, M. Taddei, B. Stecca, Targeted inhibition of Hedgehog-GLI signaling by novel acylguanidine derivatives inhibits melanoma cell growth by inducing replication stress and mitotic catastrophe, Cell Death Dis. 9 (2018) 142. DOI: 10.1038/s41419-017-0142-0.

[20] F. Manetti, H. Faure, H. Roudaut, T. Gorojankina, E. Traiffort, A. Schoenfelder, A. Mann, A. Solinas, M. Taddei, M. Ruat, Virtual screening-based discovery and mechanistic characterization of the acylthiourea MRT-10 family as smoothened antagonists, Mol. Pharmacol. 78 (2010) 658-665. doi: 10.1124/mol.110.065102.

[21] H. Roudaut, E. Traiffort, T. Gorojankina, L. Vincent, H. Faure, A. Schoenfelder, A. Mann, F. Manetti, A. Solinas, M. Taddei, M. Ruat, Identification and mechanism of action of the acylguanidine MRT-83, a novel potent Smoothened antagonist, Mol. Pharmacol. 79 (2011) 453-60. doi: 10.1124/mol.110.069708.

[22] A. Fleury, L. Hoch, M.C. Martinez, H. Faure, M. Taddei, E. Petricci, F. Manetti, N. Girard, A. Mann, C. Jacques, J. Larghero, M. Ruat, R. Andriantsitohaina, S. Le Lay, Hedgehog associated to microparticles inhibits adipocyte differentiation via a non-canonical pathway, Sci. Rep. 24 (2016) 23479. doi: 10.1038/srep23479.

[23] S. Gambassi, M. Geminiani, S.D. Thorpe, G. Bernardini, L. Millucci, D. Braconi, M. Orlandini, C.L. Thompson, E. Petricci, F. Manetti, M. Taddei, M.M. Knight, A. Santucci, Smoothened-antagonists reverse homogentisic acid-induced alterations of Hedgehog signaling and primary cilium length in alkaptonuria, J. Cell. Physiol. 232 (2017) 3103-3111. doi: 10.1002/jcp.25761.

[24] T. Gorojankina, L. Hoch, H. Faure, H. Roudaut, E. Traiffort, A. Schoenfelder, N. Girard, A. Mann, F. Manetti, A. Solinas, E. Petricci, M. Taddei, M. Ruat, Discovery, molecular and pharmacological characterization of GSA-10, a novel small-molecule positive modulator of Smoothened, Mol. Pharmacol. 83 (2013) 1020-1029. doi: 10.1124/mol.112.084590.

[25] F. Manetti, E. Petricci, A. Gabrielli, A. Mann, H. Faure, T. Gorojankina, L. Brasseur, L. Hoch, M. Ruat, M. Taddei, Design, synthesis and biological characterization of a new class of osteogenic (1*H*)-quinolone derivatives, Eur. J. Med. Chem. 121 (2016) 747-757. doi: 10.1016/j.ejmech.2016.05.062.

[26] D.A. Alonso, C. Nájera, M.C. Pacheco, Oxime-derived palladium complexes as very efficient catalysts for the Heck–Mizoroki reaction, Adv. Synth. Catal. 344 (2002) 172-183. DOI: 10.1002/1615-4169(200202)344:2<172::AID-ADSC172>3.0.CO;2-9.

[27] C.M. Alder, J.D. Hayler, R.K. Henderson, A.M. Redman, L. Shukla, L.E. Shuster, H.F. Sneddon, Updating and further expanding GSK's solvent sustainability guide. Green Chem. 18 (2016) 3879-3890. DOI: 10.1039/C6GC00611F.

[28] T. Nakamura, T. Aikawa, M. Iwamoto-Enomoto, M. Iwamoto, Y. Higuchi, M. Pacifici, N. Kinto, A. Yamaguchi, S. Noji, K. Kurisu, T. Matsuya, Induction of osteogenic differentiation by hedgehog proteins, Biochem. Biophys. Res. Commun. 237 (1997) 465-469.

[29] K.P. Williams, P. Rayhorn, G. Chi-Rosso, E.A. Garber, K.L. Strauch, G.S. Horan, J.O. Reilly, D.P. Baker, F.R. Taylor, V. Koteliansky, R.B. Pepinsky, Functional antagonists of sonic hedgehog reveal the importance of the N terminus for activity, J. Cell Sci. 112 (1999) 4405-4414.

[30] S.E Gould, J.A. Low, J.C. Marsters Jr, K. Robarge, L.L. Rubin, F.J. de Sauvage, D.P. Sutherlin, H.Wong, R.L. Yauch, Discovery and preclinical development of vismodegib, Expert Opin. Drug Discov. 9 (2014) 1-16 and references cited herein.

1) Gram-scale synthesis of Hedgehog inhibitors with an Heck coupling
2) Cell-based evaluation and ADME profiling with vismodegib as reference
3) The phenetyl analogue **5** is a safe inhibitor of a LS180 colon cancer xenograft